Available online at www.sciencedirect.com
ScienceDirect
Ceramics International 37 (2011) 2429–2435
CERAMICS INTERNATIONAL
www.elsevier.com/locate/ceramint

# The effect of interfacial bonding of calcium phosphate cements containing bio-mineralized multi-walled carbon nanotube and bovine serum albumin on the mechanical properties of calcium phosphate cements

Kah Ling Low [a], Sharif Hussein Sharif Zein [a,*], Soon Huat Tan [a], David S. McPhail [b], Aldo R. Boccaccini [b,c]

[a] School of Chemical Engineering, Engineering Campus, Universiti Sains Malaysia, Seri Ampangan, 14300 Nibong Tebal, Seberang Perai Selatan, Pulau Pinang, Malaysia
[b] Department of Materials, Imperial College London, Prince Consort Road, London SW7 2AZ, UK
[c] Institute of Biomaterials, Department of Materials Science and Engineering, University of Erlangen-Nuremberg, 91058 Erlangen, Germany

Received 8 November 2010; received in revised form 28 February 2011; accepted 24 March 2011
Available online 27 May 2011

**Abstract**

The aim of this study was to investigate the effect of adding bio-mineralized hydroxyl functionalized multi-walled carbon nanotubes (MWCNTs–OH) on the compressive strength of calcium phosphate cements (CPCs). Bovine serum albumin (BSA) was also incorporated as a protein which acts as promoter of hydroxyapatite (HA) crystal growth when bounded to CPC granules. The results show that the strong interfacial bonding of CPC/MWCNTs–OH is essential to improve the mechanical properties of CPC/bio-mineralized MWCNTs–OH/BSA composite.


*Keywords:* B. Interfaces; B. Composites; C. Mechanical properties; Hydroxyapatite

## 1. Introduction

Calcium phosphate cements (CPCs) are potential materials for use in minimal invasive surgery for bone defect repair due to their similarity to the mineral phase of bone [1]. CPCs have been developed as injectable bone substitutes (IBS) because of their biocompatibility, excellent bioactivity, self-setting characteristics, low setting temperature, adequate stiffness and easy shaping in complicated geometries [2,3]. A number of CPC products are available commercially. However, due to their limited compressive strength, the use of CPCs is restricted primarily to non-stress-bearing applications such as in maxillofacial surgery, the repair of cranial defects and dental fillings [4–6]. Therefore, new CPCs with excellent mechanical strength, enhanced bioactivity and resorbability should be developed in order to broaden the application potential to heal bone fractures and bone diseases [7].

Since the comprehensive investigation by Iijima [8], carbon nanotubes (CNTs) have been the focal point of considerable research. There is increasing interest in applications of CNTs as reinforcement in composite materials because of their excellent mechanical properties [9–12]. However, there are two main obstacles to overcome when using CNTs as reinforcing elements, which are: (i) enhancing the wettability of the CNTs surface to improve the matrix/CNT interface in order to enable efficient load transfer from the matrix to the nanotube [13] and (ii) achieving an homogeneous dispersion of CNTs in the matrix material [14]. Thus, good interfacial bonding is an essential condition in order to improve the mechanical properties of CNTs containing composites [15]. Due to the chemically inertness and highly hydrophobic nature of CNTs, modification of their surfaces is required so that efficient CNTs–matrix interactions can be created [14,16]. In particular in case of inorganic matrices, surface functionalization facilitates improved dispersion of CNTs in the ceramic or

* Corresponding author. Tel.: +60 4 599 6442; fax: +60 4 594 1013.
*E-mail address:* chhussein@eng.usm.my (S.H.S. Zein).

0272-8842/$36.00 
doi:10.1016/j.ceramint.2011.05.092

glass matrix, leading also to the achievement of an ideal interface bonding, which will be ultimately responsible for an efficient load-transfer mechanism. Despite some concerns about possible cytotoxic effects, there is an ever increasing interest in the application of functionalized CNTs in the biomedical field [17–21]. Recently, the manufacturing and properties of CNTs-reinforced hydroxyapatite (HA) ceramic composites suitable for clinical bone graft procedures have been presented [22,23]. Zhao et al. [24] reported the mineralization of chemically functionalized single walled carbon nanotubes (SWCNTs) with CPC using a variety of functionalities, including the carboxylic acid group (–COOH), the phosphonate group (diethyl methylene phosphonate ester and diethyl benzyl phosphonate amide) and the sulfonic acid group [poly(aminobenzene sulfonic acid), PABS]. These functionalities were introduced by chemical reaction and they were shown to improve the solubility of SWCNTs in water and to exert a strong effect on the mineralization of the SWCNTs with HA [24]. In related research, Wang et al. [15] have reported the reinforcement of CPC (50 wt% partially crystallized calcium phosphate (PCCP) and dicalcium phosphate anhydrous (DCPA)) with CNTs functionalized with –COOH. However, the type of CNTs used was not reported. If CPC is reinforced by bio-mineralized functionalized multi-walled carbon nanotubes (MWCNTs), a composite with higher mechanical properties and bioactivity can be obtained, which has potential application as bone repair material. In addition, results in the literature show that CNTs can be used to induce the ordered growth of a nano-HA surface layer on biomaterial surfaces for example in contact with simulated body fluid, which provides a nanostructured topography that resembles closely the surface of bone in its chemistry, crystallinity and morphology [25–27].

In our previous study, the reinforcement of CPC with 0.5 wt% as-received MWCNTs–OH and the addition of 15 wt% BSA was investigated [28]. A relatively high compressive strength was measured, as compared with CPC/BSA composites reinforced by as-received MWCNTs and MWCNTs–COOH. Thus, the aim of this study is to develop a novel CPC based composite consisting of β-tricalcium phosphate (β-TCP) and DCPA containing MWCNTs functionalized with hydroxyl ions (–OH) and bio-mineralized by treatment with SBF. Subsequently the resulting composites were incorporated with bovine serum albumin (BSA) in order to enhance crystal growth. This novel CPC composite combines the osteoconductive properties of CPCs, the excellent mechanical properties of MWCNTs–OH and the crystal growth effect induced by BSA. The interfacial bonding between MWCNTs–OH and the CPC matrix as well as the HA crystal growth in the composites were investigated and the compressive strength was measured. The new composites are proposed for applications as bone substitute materials.

## 2. Materials and methods

### 2.1. Sample preparation

Bio-mineralized MWCNTs–OH were prepared by immersing MWCNTs–OH (95% purity, diameter = 30–50 nm, length = $\sim$ 20 μm) (provided by Chinese Academic of Science, China) in simulated body fluid (SBF) for 7 days. The SBF was prepared according to the Kokubo method reported in the literature [29,30]. The product formed was washed with distilled water and filtered. Then, the product was dried in air at room temperature. Equimolar mixtures of β-TCP and DCPA (supplied by Sigma–Aldrich) were physically mixed with 15 wt% of BSA in powder form (supplied by Fluka) and with 0.5 wt % of as-received MWCNTs–OH or bio-mineralized MWCNTs–OH. De-ionized water was then added to the mixed compounds and the mixtures were blended by using a mechanical overhead stirrer in order to obtain a workable cement paste. The cement paste obtained was firmly packed into a stainless steel mold to prepare cylindrical specimens (diameter = 25 mm, height = 10 mm) for compressive strength tests. The packed stainless steel mold was wrapped with water soaked KimWipe tissue paper to prevent the sample from drying out and it was then stored in a Gyro-Rocker Incubator (Model: S170) at 37 °C and 97% humidity for 24 h. Upon removing from the incubator, the cylindrical specimens were carefully taken out from the mold. The compressive strength of the cylindrical specimens was tested using an Instron 3367 universal testing machine at a crosshead speed of 1.0 mm/min.

### 2.2. Sample characterization

The chemical and physical properties of CPC/as-received MWCNTs–OH/BSA and CPC/bio-mineralized MWCNTs–OH/BSA composites were investigated by scanning electron microscopy (SEM) and Fourier transform infrared (FTIR) spectroscopy. SEM was performed using a Leo Supra 35VP-24-58 microscope in order to investigate the microstructure and morphology of the composites. Fracture fragments were mounted on conducting carbon tape and observed using an accelerating voltage of 5 keV. FTIR was carried out on a Perkin-Elmer FTIR 2000 spectrometer over the frequency range 4000–400 $cm^{-1}$ in KBr pellets. FTIR spectroscopy was employed to characterize the presence of specific surface functional groups in the composites.

## 3. Results and discussion

### 3.1. Formulations of CPC composites

In order to achieve a controlled combination of degradation behavior and bioactivity to promote bone formation, we used β-TCP and DCPA as the main components of the CPC material [31]. As a candidate material for bone graft, β-TCP has excellent merit in bone formation [32]. Mixtures of β-TCP and DCPA for bone substitution have been used for many years [33]. It has been shown that the more slowly resorbing granules are surrounded by newly grown bone, thus providing an inverse scaffold for bone regeneration [34]. Thus, by adding β-TCP granules, the overall resorption rate of the cement can be tailored to meet specific needs and the bone formation rate can be controlled. Cements containing β-TCP and DCPA have been found to completely degrade in 16 weeks in vivo [33].

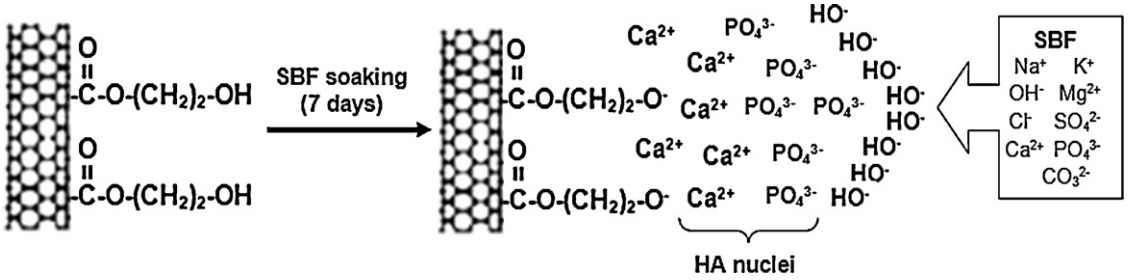


Fig. 1. Schematic representation of the process of HA growth on the surface of MWCNTs–OH when soaked in SBF. Adapted from Wang et al. [15].

In this study, β-TCP and DCPA were mixed with de-ionized water to form calcium deficient HA [$Ca_9(HPO_4)(PO_4)_5(OH)$] (CDHA). Then, this HA was mixed with as-received MWCNTs–OH or with bio-mineralized MWCNTs–OH and incorporated with BSA to form CPC/as-received MWCNTs–OH/BSA and CPC/bio-mineralized MWCNTs–OH/BSA composites. The schematic diagram shown in Fig. 1 illustrates the precipitation of HA on the surface of bio-mineralized MWCNTs–OH by immersion in SBF, as suggested by Wang et al. [15]. The –OH groups react with the –OH ions in SBF to produce a negatively charged surface with the functional group $–COO(CH_2)_2O^-$, as shown in Eq. (1):

$$-COO(CH_2)_2OH + OH^- \rightarrow -COO(CH_2)_2O^- + H_2O \quad (1)$$

In SBF, activated $–COO(CH_2)_2OH$ surfaces can act as nucleation sites for HA [15,35]. Then $Ca^{2+}$ in the SBF solution can be attracted to the negatively charged surface site of MWCNTs–OH. The attachment of $PO_4^{3-}$ from the HA nuclei at the $Ca^{2+}$ accumulated sites result in a precursor cluster of calcium phosphate. Thus, HA nuclei can precipitate on the surface of the MWCNTs–OH when immersed in SBF, which will form a suitable interfacial bonding between the bio-mineralized MWCNTs–OH and the CPC matrix. Besides, there is a crystallization process taking place when bio-mineralized MWCNTs–OH are mixed with β-TCP, DCPA and BSA to form CPC/bio-mineralized MWCNTs–OH/BSA composite. In this process, effective interfacial bonding is expected between the bio-mineralized MWCNTs–OH and the CPC matrix while BSA can promote HA crystal growth. The consequence of these microstructural reactions should lead to the improvement of the compressive strength of the composites.

Furthermore, it is well-known that SBF with ion concentrations similar to those of the inorganic constituents of human blood plasma is able to act as a medium for the development of a low crystallized HA similar to the mineral phase of bone on substrates of different materials [36–39]. It is likely that this crystallized HA layer formed on the MWCNTs–OH surfaces will further contribute to improvement of the mechanical strength of the composites.

### 3.2. Compressive Strength

Fig. 2 shows the effects of as-received and bio-mineralized MWCNTs–OH on the compressive strength of CPC compo-

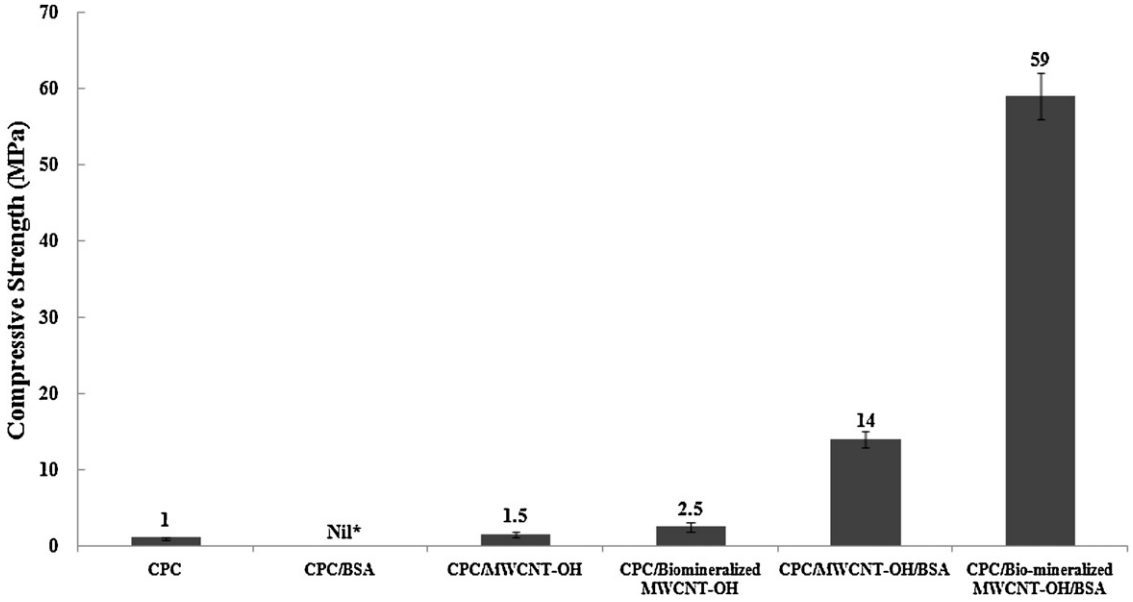


Fig. 2. Compressive strength of CPC modified by as-received MWCNTs–OH and bio-mineralized MWCNTs–OH and with addition of BSA (No. of samples, $n = 2$). *Note that the compressive strength of the CPC/BSA composite (without MWCNTs) could not be measured because the composite was too weak to form the required specimen shape for the compressive test purpose.

sites. It was found that with addition of as-received MWCNTs–OH, the compressive strength of pure CPC composite significantly increased, from $1.0 \pm 0.2$ MPa to $1.5 \pm 0.3$ MPa. The compressive strength of CPC composites is further improved from $1.0 \pm 0.2$ MPa to $2.5 \pm 0.7$ MPa, when reinforced with bio-mineralized MWCNTs–OH. Moreover, even if only two specimens were tested per condition investigated, it could be confirmed that when BSA is added, the compressive strength of CPC/as-received MWCNTs–OH composite significantly increased to $14 \pm 3$ MPa. In addition, the compressive strength of CPC/bio-mineralized MWCNTs–OH/BSA composite significantly increased to $59 \pm 3$ MPa, as compared to CPC/as-received MWCNTs–OH/BSA composite.

As discussed above, HA crystals precipitated on the surface of bio-mineralized MWCNTs–OH should induce strong interfacial bonding between HA nuclei and bio-mineralized MWCNTs–OH. A strong interfacial bonding is a necessary condition for improving the mechanical properties of composites, in order to achieve load transfer across the MWCNTs–matrix interface [40]. Because of the chemically inertness and the highly hydrophobic nature of the MWCNTs–OH [16], as-received MWCNTs–OH did not exhibit a favorable wettability for dispersion in CPC matrices and there was no strong interfacial bonding between the as-received MWCNTs–OH and the CPC matrix. Thus, MWCNTs–OH in the as-received condition cannot be used as a stable reinforcement element in CPC. In contrast, there was an interfacial bonding formed between the bio-mineralized MWCNTs–OH and the CPC matrix. This interface favors the load transfer between the bio-mineralized MWCNTs–OH and the matrix leading to improved mechanical properties.

Furthermore, the improvement in the mechanical properties with addition of BSA can be explained by considering that appropriate amounts of BSA are capable of promoting crystal growth in the CPC matrix [41,42]. At low concentrations (<10 g/l), BSA has been hypothesized to stabilize nuclei and promote growth of octacalcium phosphate crystals while at higher concentrations of BSA, the crystal growth seems to be impeded by excessive BSA coverage [41]. The protein contains both positively and negatively charged residues [43]. The arrangement of these charges, as well as the complementarities between the charged groups on the protein and the growing apatite surfaces, may influence crystal growth behavior and also lead to more cohesive cements for higher BSA contents [42,44]. In this study, it was hypothesized that BSA would promote HA crystal growth and contribute to the increase of the compressive strength, which was confirmed by the experiments (Fig. 2).

### 3.3. Microstructural analysis

#### 3.3.1. Scanning electron microscopy (SEM)

Fig. 3 shows SEM images of the composite microstructures. In general, different morphologies of the HA crystal structures of CPC/as-received MWCNTs–OH/BSA and CPC/bio-mineralized MWCNTs–OH/BSA composites were observed, as shown in Fig. 3(a and b), respectively. These different microstructures may be the result of the effect of the different

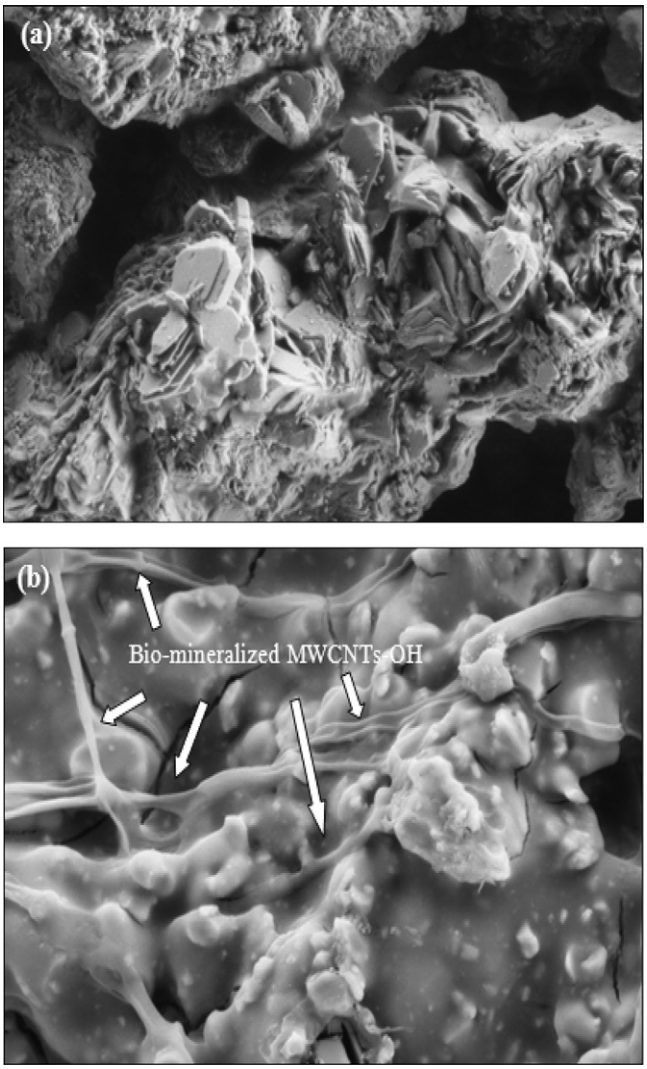


Fig. 3. SEM micrographs of CPC composite morphologies; (a) CPC/as-received MWCNTs–OH/BSA and (b) CPC/bio-mineralized MWCNTs–OH/BSA composites.

interfacial bonding between as-received MWCNTs–OH and bio-mineralized MWCNTs–OH with the CPC matrix and the effect of the BSA for the HA crystal growth. These differences result in the marked variation in compressive strength values (Fig. 2). Referring to the morphologies of HA crystals obtained by Xu et al. [45,46], it is suggested that HA crystals are grown in CPC/as-received MWCNTs–OH/BSA and CPC/bio-mineralized MWCNTs–OH/BSA composites as a result of BSA addition. Fig. 3(a) shows that well-packed HA crystals of plate-like shape and clusters are grown in CPC/as-received MWCNTs–OH/BSA composite. It is hypothesized that this particular microstructure led to increase compressive strength of these composites. However, the interfacial bonding between as-received MWCNTs–OH and CPC matrix is weaker than that of bio-mineralized MWCNTs–OH, as discussed previously. Moreover, in the SEM image of the CPC/bio-mineralized MWCNTs–OH/BSA composite shown in Fig. 3(b), a bio-mineralized MWCNTs–OH well adhered to the CPC matrix can be observed, which is the result of the HA precipitated on

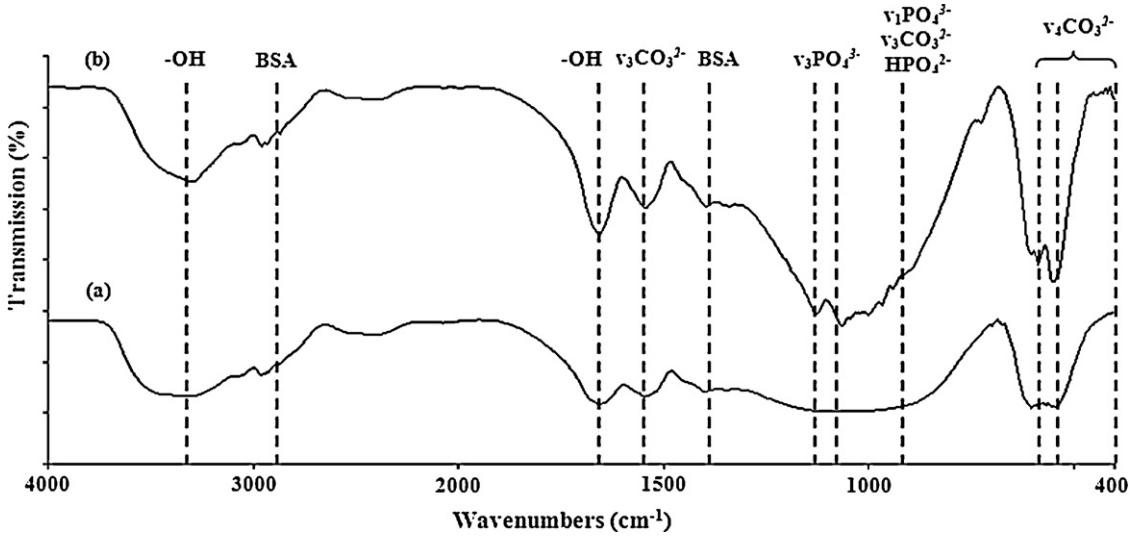


Fig. 4. FTIR patterns; (a) CPC/as-received MWCNTs–OH/BSA and (b) CPC/bio-mineralized MWCNTs–OH/BSA composites.

the outer wall of the MWCNTs–OH. It is suggested that the finer HA crystals, grown in the CPC matrix and linked with the bio-mineralized MWCNTs–OH, are responsible for the higher compressive strength of CPC/bio-mineralized MWCNTs–OH/BSA composite in comparison to CPC/as-received MWCNTs–OH/BSA composite.

### 3.3.2. *Fourier transformed infrared (FTIR) spectroscopy*

Fig. 4(a and b) illustrates the FTIR results on CPC/as-received MWCNTs–OH/BSA and CPC/bio-mineralized MWCNTs–OH/BSA composites, respectively. The spectra show absorption bands at 3297–3307 $cm^{-1}$ which correspond to the strong characteristic peak of stretching mode of –OH [47,48]. The peaks pertaining to the HA phase are –OH bands at 3302 $cm^{-1}$ and 3307 $cm^{-1}$. The characteristic bending mode of intercalated water can be observed at 1655–1656 $cm^{-1}$ [47]. The phosphate band derived from the P–O asymmetric stretching mode ($v_1$) of the $PO_4^{3-}$ group was identified in the region 943–1128 $cm^{-1}$, indicating a deviation of phosphate ions from their ideal tetrahedral structure [47,48]. The absorption bands appearing at about 400 to 600 $cm^{-1}$ can be attributed to the triple ($v_3$) 548, 587 and 603 and double ($v_2$)-degenerated fundamental bending mode of the $PO_4^{3-}$ functional group [47,48]. The bands observed at 1543 $cm^{-1}$ ($v_3$ mode) and 1546 $cm^{-1}$ ($v_3$ mode) can be assigned to the $CO_3^{2-}$ group [49]. The typical absorption bands of BSA are indicated at 2900 $cm^{-1}$ and 1400 $cm^{-1}$ [50]. As a result, all the bands discussed above and also their positions in the FTIR spectra confirm the formation of HA in both CPC/as-received MWCNTs–OH/BSA and CPC/bio-mineralized MWCNTs–OH/BSA composites. However, there are significant sharper P–O bands ($v_3$ mode) at 1065–1100 $cm^{-1}$ for the CPC/bio-mineralized MWCNTs–OH/BSA composite, which could prove that HA particles precipitated on the outer wall of

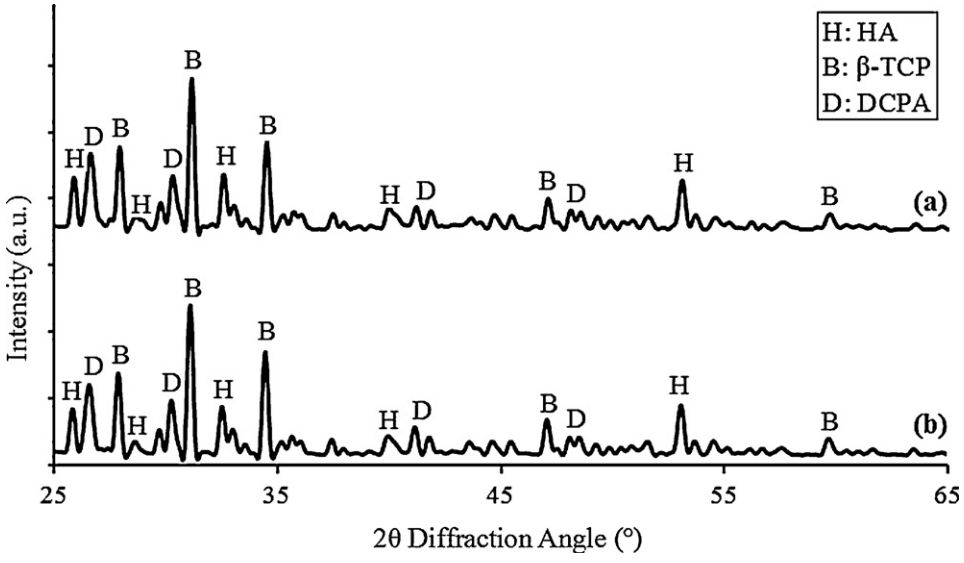


Fig. 5. X-ray diffraction patterns of the investigated samples; (a) CPC/MWCNTs–OH/BSA and (b) CPC/bio-mineralized MWCNTs–OH/BSA composites.

bio-mineralized MWCNTs–OH [15]. This result also supports the hypothesis about the forming of interfacial bonding between bio-mineralized MWCNTs–OH and HA, which leads to the relatively high compressive strength of CPC/bio-mineralized MWCNTs–OH/BSA composite compared with CPC/as-received MWCNTs–OH/BSA composite.

### 3.3.3. X-ray diffraction (XRD)

Fig. 5 presents typical XRD patterns of the CPC/as-received MWCNTs–OH/BSA and CPC/bio-mineralized MWCNTs–OH/BSA composites. Diffraction peaks corresponding to HA crystalline phase were found at $2\theta$ angles of 26, 29, 32, 40 and 53°. The presence of an intense diffraction peak at $2\theta = 26^\circ$ reveals the growth of HA crystal along the *c*-axis [51,52]. These XRD results confirming the presence of HA can be correlated with the crystal morphology observed in the SEM images (Fig. 3(a and b)). However, the XRD analysis also revealed two extra phases of the starting materials corresponding to β-TCP and DCPA, suggesting that the reaction to form CPC is incomplete. The incomplete reaction might be due to several factors such as the liquid to powder ratio used, the hydration time and the hydration environment. Considered in conjunction, the SEM, FTIR and XRD results showed that the investigated CPC composites developed a crystalline HA phase, which is in its chemical and crystallographic composition similar to the mineral phase of bone [53].

## 4. Conclusions

MWCNTs–OH was soaked in SBF for 7 days to synthesize bio-mineralized MWCNTs–OH. The bio-mineralized MWCNTs–OH was homogenously mixed with CPC and BSA to form CPC/bio-mineralized MWCNTs–OH/BSA composites. The strong interfacial bonding formed between bio-mineralized MWCNTs–OH and CPC is suggested to have led to compressive strength values significantly higher than those of CPC/as-received MWCNTs–OH/BSA composite. SEM, FTIR and XRD results showed that a HA layer precipitated on the surface of the bio-mineralized MWCNTs–OH, which should lead to a strong interface. Hence, bio-mineralized MWCNTs–OH can play a reinforcement role in the CPC matrix through the formation of interfacial bonding between HA nuclei and –OH groups of MWCNTs–OH. Due to concerns about the biocompatibility and possible toxicity of CNTs for their use as biomaterials [21], further research should focus on in vitro cell-biological investigations and on the in vivo performance of the novel CPC composites developed here. Significant work must be carried out to improve the properties of the composites and to assess their bioactivity and toxicity before they can be considered for clinical applications.

## Acknowledgements

The work was financially supported by the British Council through the UK's Prime Minister's Initiative for International Education (PMI2) Connect scheme and USM-RU grant. Kah Ling Low also acknowledges the USM Fellowship for the support of her studies.

## References

[1] H.P. Yuan, Y.B. Li, J.D. de Bruijn, K. de Groot, X.D. Zhang, Tissue responses of calcium phosphate cement: a study in dogs, Biomaterials 21 (2000) 1283–1290.
[2] X.P. Wang, J.D. Ye, Y.J. Wang, L. Chen, Self-setting properties of a β-dicalcium silicate-reinforced calcium phosphate cement, J. Biomed. Mater. Res. B 82 (1) (2007) 93–99.
[3] E. Fernandez, Bioactive bone cements, in: Metin Akay (Ed.), Wiley Encyclopedia of Biomedical Engineering, John Wiley & Sons, Inc., NY, 2006, pp. 1–9.
[4] C.D. Friedman, P.D. Costantino, S. Takagi, L.C. Chow, Bone-source™ hydroxyapatite cement: a novel biomaterial for craniofacial skeletal tissue engineering and reconstruction, J. Biomed. Mater. Res. B: Appl. Biomater. 43 (1998) 428–432.
[5] J.P. Schmitz, J.O. Hollinger, S.B. Milam, Reconstruction of bone using calcium phosphate bone cements: a critical review, J. Oral Maxillofac. Surg. 57 (1999) 1122–1126.
[6] M. Bohner, Calcium orthophosphates in medicine: from ceramics to calcium phosphate cements, Injury 31 (2000) SD37–SD47.
[7] K.L. Low, S.H. Tan, S.H.S. Zein, J.A. Roether, V. Mouriño, A.R. Boccaccini, Review: calcium phosphate-based composites as injectable bone substitute materials, J. Biomed. Mater. Res. B: Appl. Biomater. 94B (2010) 273–286.
[8] S. Iijima, Helical microtubules of graphitic carbon, Nature 354 (1991) 56–58.
[9] M.M.J. Treacy, T.W. Ebbesen, J.M. Gibson, Exceptionally high Young's modulus observed for individual carbon nanotubes, Nature 381 (6584) (1996) 678–680.
[10] E.W. Wong, P.E. Sheehan, C.M. Lieber, Nanobeam mechanics: elasticity, strength, and toughness of nanorods and nanotubes, Science 277 (1997) 1971–1975.
[11] M.F. Yu, B.S. Files, S. Arepalli, R.S. Ruoff, Tensile loading of ropes of single wall carbon nanotubes and their mechanical properties, Phys. Rev. Lett. 84 (2000) 5552–5555.
[12] F.H. Gojny, J. Nastalczyk, Z. Roslaniec, K. Schulte, Surface modified multi-walled carbon nanotubes in CNT/epoxy-composites, Chem. Phys. Lett. 370 (2003) 820–824.
[13] K. Hernadi, E. Ljubovi, J.W. Seo, L. Forró, Synthesis of MWNT based composite materials with inorganic coating, Acta Mater. 51 (2003) 1447–1452.
[14] J. Cho, A.R. Boccaccini, M.S.P. Shaffer, Ceramic matrix composites containing carbon nanotubes, J. Mater. Sci. 44 (2009) 1934–1951.
[15] X.P. Wang, J.D. Ye, Y.J. Wang, L. Chen, Reinforcement of calcium phosphate cement by bio-mineralized carbon nanotube, J. Am. Ceram. Soc. 90 (3) (2007) 962–964.
[16] T. Seeger, T. Köhler, T. Frauenheim, N. Grobert, M. Rühle, M. Terrones, G. Seifert, Nanotube composites: novel $SiO_2$ coated carbon nanotubes, Chem. Commun. 7 (1) (2002) 34–35.
[17] M.P. Mattson, R.C. Haddon, A.M. Rao, Molecular functionalization of carbon nanotubes and use as substrates for neuronal growth, J. Mol. Neurosci. 14 (2000) 175–182.
[18] H. Hu, Y.C. Ni, V. Montana, R.C. Haddon, V. Parpura, Chemically functionalized carbon nanotubes as substrates for neuronal growth, Nano Lett. 4 (2004) 507–511.
[19] H. Hu, Y.C. Ni, S.K. Mandal, V. Montana, B. Zhao, R.C. Haddon, V. Parpura, Polyethyleneimine functionalized single-walled carbon nanotubes as a substrate for neuronal growth, J. Phys. Chem. B 109 (10) (2005) 4285–4289.
[20] P.Z. Laura, B. Zhao, H. Hu, R.C. Haddon, Bone cell proliferation on carbon nanotubes, Nano Lett. 6 (3) (2006) 562–567.
[21] B.S. Harrison, A. Attala, Carbon nanotube applications for tissue engineering, Biomaterials 28 (2007) 344–353.
[22] C. Kealley, M. Elcombe, A.V. Riessen, M.B.N. Besi, Development of carbon nanotube-Reinforced hydroxyapatite bioceramics, Physica B 385–386 (2006) 496–498.

[23] A.A. White, S.M. Best, I.A. Kinloch, Hydroxyapatite-carbon nanotube composites for biomedical applications: a review, Int. J. Appl. Ceram. Technol. 4 (2007) 1–13.
[24] B. Zhao, H. Hu, S.K. Mandal, R.C. Haddon, A bone mimic based on the self-assembly of hydroxyapatite on chemically functionalized single-walled carbon nanotubes, Chem. Mater. 17 (12) (2005) 3235–3241.
[25] T. Akasaka, F. Watari, Y. Sato, K. Tohji, Apatite formation on carbon nanotubes, Mater. Sci. Eng. C 26 (2006) 675–678.
[26] S. Aryal, S.R. Bhattarai, K.C. Remant Bahadur, M.S. Khil, D.R. Lee, H.Y. Kim, Carbon nanotubes assisted biomimetic synthesis of hydroxyapatite from simulated body fluid, Mater. Sci. Eng. A 426 (2006) 202–207.
[27] A.R. Boccaccini, F. Chicatun, J. Cho, O. Bretcanu, J.A. Roether, S. Novak, Q.Z. Chen, Carbon nanotube coatings on bioglass-based tissue engineering scaffold, Adv. Funct. Mater. 17 (2007) 2815–2822.
[28] K.K. Chew, K.L. Low, S.H.S. Zein, D.S. McPhail, L.C. Gerhardt, J.A. Roether, A.R. Boccaccini, Reinforcement of calcium phosphate cement with multi-walled carbon nanotubes and bovine serum albumin for injectable bone substitute applications, J. Mech. Behav. Biomed. Mater. 4 (3) (2011) 331–339.
[29] O. Chikara, How to prepare the simulated body fluid (SBF) and its related solutions, proposed by Kokubo and his colleagues. Available at: http://mswebs.naist.jp/LABs/tanihara/ohtsuki/SBF/index.html, (accessed January 2010).
[30] T. Kokubo, H. Kushitani, S. Sakka, T. Kitsugi, T. Yamamuro, Solutions able to reproduce in vivo surface-structure changes in bioactive glass–ceramic A-W, J. Biomed. Mater. Res. 24 (1990) 721–734.
[31] M. Kitamura, C. Ohtsuki, H. Iwasaki, S. Ogata, M. Tanihara, T. Miyazaki, The controlled resorption of porous alpha-tricalcium phosphate using a hydroxypropylcellulose coating, J. Mater. Sci. Mater. Med. 15 (2004) 1153–1158.
[32] N.E. Epstein, A preliminary study of the efficacy of beta tricalcium phosphate as a bone expander for instrumented posterolateral lumbar fusions, J. Spinal Disord. Tech. 19 (2006) 424–429.
[33] Y. Weitao, K. Kangmei, J. Anmin, An injectable cement: synthesis, physical properties and scaffold for bone repair, J. Postgrad. Med. 53 (2007) 34–38.
[34] A. Gisep, R. Wieling, M. Bohner, S. Matter, E. Schneider, B. Rahn, Resorption patterns of calcium phosphate cements in bone, J. Biomed. Mater. Res. A 66 (2003) 532–540.
[35] C.S. Wu, Antibacterial and static dissipating composites of poly(butylenes adipate-co-terephthalate) and multi-walled carbon nanotubes, Carbon 47 (2009) 3091–3098.
[36] T. Kokubo, Surface chemistry of bioactive glass–ceramics, J. Non-Cryst. Solids 120 (1990) 138–151.
[37] C. Ohtsuki, T. Kokubo, T. Yamamuro, Mechanism of apatite formation on $CaO–SiO_2–P_2O_5$ glasses in a simulated body fluid, J. Non-Cryst. Solids 143 (1992) 84–92.
[38] H. Ylanen, K.H. Karlsson, A. Itala, H.T. Aro, Effect of immersion in SBF on porous bioactive bodies made by sintering bioactive glass microspheres, J. Non-Cryst. Solids 275 (9) (2000) 107–115.
[39] E.I. Dorozhkina, M. Epple, S.V. Dorozhkin, Biomimetic crystallization of calcium phosphates under constant conditions from the revised SBF, Bioceramics 15 (240–242) (2003) 85–88.
[40] L.P. Zhao, L. Gao, Novel in situ synthesis of MWNTs-hydroxyapatite composites, Carbon 42 (2004) 423–460.
[41] C. Combes, C. Rey, M. Freche, In vitro crystallization of octacalcium phosphate on type I collagen: influence of serum albumin, J. Mater. Sci. Mater. Med. 10 (3) (1999) 153–160.
[42] E.M. Burke, Y. Guo, L. Colon, M. Rahima, A. Veis, G.H. Nancollas, Influence of polyaspartic acid and phosphophoryn on octacalcium phosphate growth kinetics, Colloids Surf. B: Biointerfaces 17 (1) (2000) 49–57.
[43] T. Peters, All about Albumin: Biochemistry, Genetics and Medical Applications, Academic Press, San Diego, CA, 1996.
[44] A. Zieba, G. Sethuraman, F. Perez, G.H. Nancollas, D. Cameron, Influence of organic phosphonates on hydroxyapatite crystal growth kinetics, Langmuir 12 (11) (1996) 2853–2888.
[45] H.H.K. Xu, M.D. Weir, E.F. Burguera, A.M. Fraser, Injectable and macroporous calcium phosphate cement scaffold, Biomaterials 27 (24) (2006) 4279–4287.
[46] H.H.K. Xu, M.D. Weir, C.G. Simon, Injectable and strong nano-apatite scaffolds for cell/growth factor delivery and bone regeneration, Dent. Mater. 24 (9) (2008) 1212–1222.
[47] M.P. Mahabole, R.C. Aiyer, C.V. Ramakrishna, B. Sreedhar, R.S. Khairnar, Synthesis, characterization and gas sensing property of hydroxyapatite ceramic, Bull. Mater. Sci. 28 (6) (2005) 535–545.
[48] W. Janusz, E. Skwarek, S. Pasieczna-Patkowska, A. Slosarczyk, Z. Paszkiewicz, A. Rapacz-Kmita, A study of surface properties of calcium phosphate by means of photoacoustic spectroscopy (FT-IR/PAS), potentiometric titration and electrophoretic measurements, Eur. Phys. J. Special Top. 154 (2008) 329–333.
[49] M. Komath, H.K. Varma, R. Sivakumar, On the development of an apatitic calcium phosphate bone cement, Bull. Mater. Sci. 23 (2) (2000) 135–140.
[50] S.V. Dorozhkin, E.I. Dorozhkina, The influence of bovine serum albumin on the crystallization of calcium phosphates from a revised simulated body fluid, Colloids Surf. A: Physicochem. Eng. Aspects 215 (2003) 191–199.
[51] M. Cao, Y. Wang, C. Guo, Y. Qi, C. Hu, Preparation of ultrahigh aspect-ratio hydroxyapatite nanofibers in reverse micelles under hydrothermal conditions, Langmuir 20 (2004) 4784–4786.
[52] R. Murugan, S. Ramakrishna, Crystallographic study of hydroxyapatite bioceramics derived from various sources, Cryst. Growth Des. 5 (2005) 111–112.
[53] M. Bohner, G. Baroud, Injectability of calcium phosphate pastes, Biomaterials 26 (2005) 1553–1563.